



HAL
open science

Monitoring Water Levels and Discharges Using Radar Altimetry in an Ungauged River Basin: The Case of the Ogooué

Sakaros Bogning, Frédéric Frappart, Fabien Blarel, Fernando Nino, Gil Mahe, Jean-Pierre Bricquet, F. Seyler, Raphaël Onguéné, Jacques Etame, Marie-Claire Paiz, et al.

► **To cite this version:**

Sakaros Bogning, Frédéric Frappart, Fabien Blarel, Fernando Nino, Gil Mahe, et al.. Monitoring Water Levels and Discharges Using Radar Altimetry in an Ungauged River Basin: The Case of the Ogooué. *Remote Sensing*, 2018, 10 (3), pp.350. 10.3390/rs10020350 . hal-01903847

HAL Id: hal-01903847

<https://hal.umontpellier.fr/hal-01903847v1>




Submitted on 24 Oct 2018

HAL is a multi-disciplinary open access archive for the deposit and dissemination of scientific research documents, whether they are published or not. The documents may come from teaching and research institutions in France or abroad, or from public or private research centers.

L'archive ouverte pluridisciplinaire **HAL**, est destinée au dépôt et à la diffusion de documents scientifiques de niveau recherche, publiés ou non, émanant des établissements d'enseignement et de recherche français ou étrangers, des laboratoires publics ou privés.

Article

Monitoring Water Levels and Discharges Using Radar Altimetry in an Ungauged River Basin: The Case of the Ogooué

Sakaros Bogning^{1,2,3,*}, Frédéric Frappart^{3,4}, Fabien Blarel³, Fernando Niño³ , Gil Mahé⁵ , Jean-Pierre Bricquet⁵, Frédérique Seyler⁶ , Raphaël Onguéné², Jacques Etamé¹, Marie-Claire Paiz⁷ and Jean-Jacques Braun⁴

¹ Département de Sciences de la Terre, Université de Douala, BP 24 157 Douala, Cameroun; etame.jacques@yahoo.fr

² Jeune Equipe Associée à l'IRD—Réponse du Littoral Camerounais aux Forçages Océaniques Multi-Échelles (JEA-RELIFOME), Université de Douala, BP 24 157 Douala, Cameroun; ziongra@yahoo.fr

³ LEGOS, Université de Toulouse, CNES, CNRS, IRD, UPS OMP, 14 Av. E. Belin, 31400 Toulouse, France; frederic.frappart@legos.obs-mip.fr (F.F.); fabien.blarel@legos.obs-mip.fr (F.B.); fernando.nino@ird.fr (F.N.)

⁴ GET, Université de Toulouse, CNRS, IRD, UPS OMP, 14 Av. E. Belin, 31400 Toulouse, France; jjbraun1@gmail.com

⁵ HydroSciences Montpellier, Université de Montpellier, CNRS, IRD, 300 Av. Pr E. Jeanbrau, 34090 Montpellier, France; gil.mahe@ird.fr (G.M.); jean-pierre.bricquet@ird.fr (J.-P.B.)

⁶ ESPACE-DEV, Université de Montpellier, IRD, Université des Antilles, Université de Guyane, Université de La Réunion, Maison de la Télédétection, 500 Rue J-F. Breton, 34093 Montpellier, France; frederique.seyler@ird.fr

⁷ The Nature Conservancy Gabon Program Office, Lot 114 Haut de Gué-Gué, 13553 Libreville, Gabon; mcpaiz@tnc.org

* Correspondence: sakaros.bogning@legos.obs-mip.fr; Tel.: +33-561-332-970

Received: 30 January 2018; Accepted: 22 February 2018; Published: 24 February 2018

Abstract: Radar altimetry is now commonly used for the monitoring of water levels in large river basins. In this study, an altimetry-based network of virtual stations was defined in the quasi ungauged Ogooué river basin, located in Gabon, Central Africa, using data from seven altimetry missions (Jason-2 and 3, ERS-2, ENVISAT, Cryosat-2, SARAL, Sentinel-3A) from 1995 to 2017. The performance of the five latter altimetry missions to retrieve water stages and discharges was assessed through comparisons against gauge station records. All missions exhibited a good agreement with gauge records, but the most recent missions showed an increase of data availability (only 6 virtual stations (VS) with ERS-2 compared to 16 VS for ENVISAT and SARAL) and accuracy (RMSE lower than 1.05, 0.48 and 0.33 and R^2 higher than 0.55, 0.83 and 0.91 for ERS-2, ENVISAT and SARAL respectively). The concept of VS is extended to the case of drifting orbits using the data from Cryosat-2 in several close locations. Good agreement was also found with the gauge station in Lambaréné (RMSE = 0.25 m and $R^2 = 0.96$). Very good results were obtained using only one year and a half of Sentinel-3 data (RMSE < 0.41 m and $R^2 > 0.89$). The combination of data from all the radar altimetry missions near Lambaréné resulted in a long-term (May 1995 to August 2017) and significantly improved water-level time series ($R^2 = 0.96$ and RMSE = 0.38 m). The increase in data sampling in the river basin leads to a better water level peak to peak characterization and hence to a more accurate annual discharge over the common observation period with only a $1.4 \text{ m}^3 \cdot \text{s}^{-1}$ difference (i.e., 0.03%) between the altimetry-based and the in situ mean annual discharge.

Keywords: altimetry; water level; discharge

1. Introduction

Inland waters have a crucial role in the Earth's water cycle through complex processes at interfaces with the atmosphere and oceans. They also strongly influence socio-economic practices through their impacts on primary needs, agricultural and industrial activities [1]. Recent and future global changes and increase of population will intensify the stress on water resources [2,3]. However, in many parts of the world, reliable field measurements of water level and water discharge are either completely unavailable or difficult to access for addressing integrated water resource management, use in operational flood forecasting or disaster mitigation [4,5]. In the large rainforest of Central Africa, hosting the Congo river basin and associated small neighboring river basins, the number of hydrological stations has dramatically dropped off because of the irregular maintenance of stations; furthermore, the spatial distribution of the stations often hinder the effectiveness of the network [6].

Spaceborne radar altimetry, although originally designed for the study of ocean topography by continuously measuring the distance between the Earth's surface and the sensor onboard the satellite [7], has proved to be very useful for continental hydrology [8]. In spite of limitations over land, radar altimetry has demonstrated a strong capability to accurately retrieve water levels of large lakes and enclosed seas where the observed surfaces are sufficiently homogeneous [9,10] but also in large river basins where the cross-sections between river and altimetry ground-tracks can reach several kilometers [11,12]. These early results were obtained using Geosat and Topex/Poseidon data processed with the Ocean retracking algorithm. With the launch of ENVISAT in 2002, other retracking algorithms started to be commonly used for processing radar altimetry data. Among them, the Offset Center Of Gravity (OCO_G, also known as Ice-1) was found to provide, most of the times, the best results for the determination of river water stages [13]. Combined with availability of land dedicated corrections of the ionosphere and the wet troposphere delays and improvements in the data processing, this allowed the generalization of the use of radar altimetry for the monitoring of inland waters. Currently, all these improvements allow detection of water bodies of a few or below one hundred meters of width (e.g., [14–16]).

With the decrease in number and availability of river discharges around the world, altimetry-based water stages are used to estimate river discharges among several other techniques based on remote sensing [17]. Among them, some commonly used are (i) the application of either power law or a polynomial relationship between stage and discharge (rating curve) to altimetry-based water stages [18–21], (ii) the use of flood routing and hydrodynamics models to derive rating curves under altimetry ground-tracks [22–24], (iii) the calibration of hydrodynamics and hydrological models using altimetry-based water stages [25–29].

This study presents the multi-mission altimetry-based hydrological network setup in the Ogooué River Basin (ORB) to provide a continuous water stage and discharge monitoring in this almost ungauged basin. It aims at answering the following questions:

- what are the performances of the different altimetry missions, from ERS-2 to Sentinel-3A, to retrieve water levels?
- how does the combination of data from several altimetry virtual stations improve the retrieval of the annual discharge in the ORB?

2. Study Area

The Ogooué River is the largest Gabonese river. Its length is about 900 km from its source in the Mounts Ntalé, in Congo, at an altitude close to 840 m.a.s.l. to its mouth in the southern part of the Atlantic coast of Gabon. The Ogooué river flows northwestward in upstream until the confluence with the Ivindo and southwestward from the confluence with the Ivindo river to a 100 km long and 100 km width delta it forms in the south of Port Gentil where it discharges into the Atlantic ocean [30]. The Ogooué river basin (ORB) is located between 9° and 15°E, and 3°S and 2.5°N (Figure 1) stretching

on about 80% of the total area of Gabon and It is bounded on the east by the Congo basin, on the south by the Niari and Nyanga basins, on the west and north-west by the coastal river basins [31].

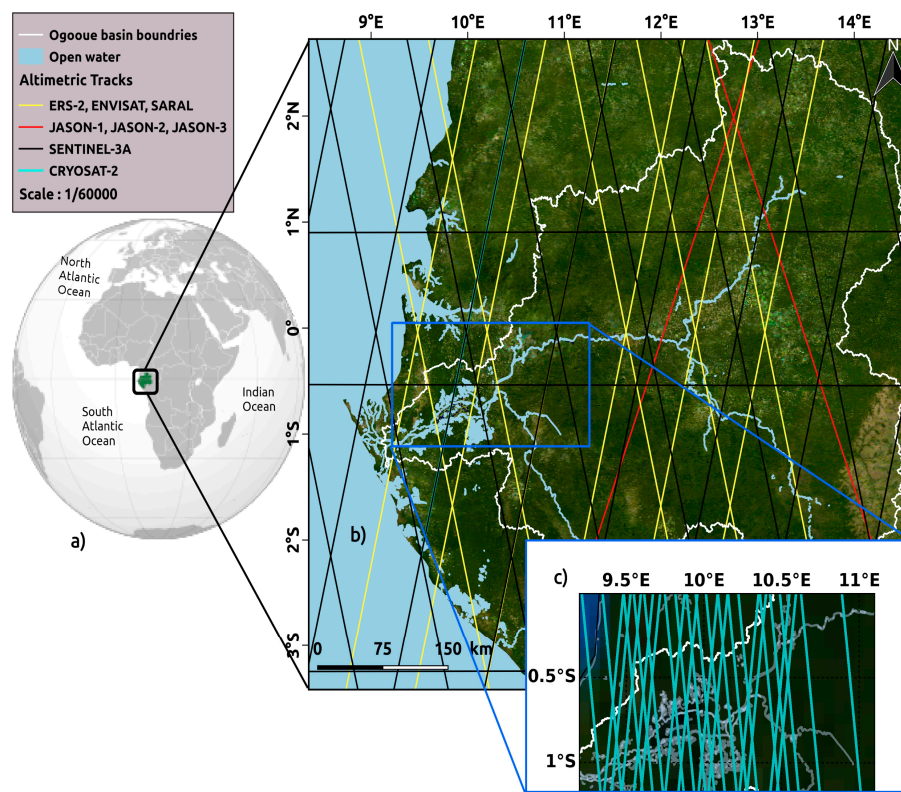


Figure 1. (a) Location of the Ogooué River Basin in Gabon in Equatorial Africa. (b) In this basin, delineated with a white line, the Ogooué and its major tributaries appear in light blue. Altimetry tracks are represented in red for the missions on a 10-day repeat cycle on their nominal track (Jason-1/2/3), in black for Sentinel-3A on its nominal track (27-day repeat cycle), in yellow for the missions on a 35-day repeat cycle on their nominal track (ERS-2/ENVISAT/SARAL), (c) zoom of the downstream of the Ogooué River Basin with altimetric tracks of Cryosat-2 on its nominal track (369-day repeat cycle) in cyan lines.

Due to its location crossing the Equator, the ORB receives the largest annual precipitation in Africa (1600–2200 mm yr⁻¹), making the annual discharge of the river of 4750 m³·s⁻¹, the third along the African West Coast after the Congo River (40,000 m³·s⁻¹) and the Niger River (5590 m³·s⁻¹) [30,32]. The annual variation of the discharge of the Ogooué river passes by two maximum : in spring and autumn corresponding to the rainy seasons [31]. On the ORB at Lambaréné, before the 1970's, river discharge of spring floods were equivalent to those of the autumn floods. After the 1970's, spring floods differ significantly from autumn floods with differences between 2000 and 3000 m³·s⁻¹ [33].

3. Datasets

3.1. Radar Altimetry Data

Radar altimetry data used in this study comes from the measurements on the nominal orbit of the following missions: Jason-2 (06/2008–10/2016), Jason-3 (since 01/2016), ERS-2 (06/1995–07/2003), ENVISAT (06/2002–10/2010), SARAL (02/2013–07/2016), Sentinel-3A (since 02/2016) and Cryosat-2 (since 04/2010—operating in low resolution mode—LRM), but also from the second (drifting) orbit of ENVISAT (10/2010–06/2012). The Jason missions have a 10-day, ERS-2, ENVISAT and SARAL a 35-day, Cryosat-2 and 369-day and Sentinel-3A a 27-day repeat-periods. Jason-2 and Jason-3 data

come from Geophysical Data Records (GDRs) D, GDR v2.1 for ENVISAT, GDR T for SARAL, GDR C for Cryosat-2 and GDR ESA IPF 06.07 land products for Sentinel-3A delivered by CNES/ESA/NASA processing centers. These data were made available by Centre de Topographie des Océans et de l'Hydrosphère (CTOH) [34]. ERS-2 data were reprocessed by CTOH to ensure the continuity with ENVISAT for land studies [35].

3.2. In Situ Water Levels and Discharges

Long-term datasets of field measured water level and discharge are not available in the ORB since it was completely ungauged between the 1980s and 2001 [31]. Only the Lambaréné gauge station gathered data from July 2001 to September 2017, sometimes with non operating periods up to a month. These in situ data of water level (collected at Lambaréné by the Société de l'Énergie et de l'Eau du Gabon, SEEG) were used to calculate the river discharge, using a historical calibration formula provided by the HydroSciences Montpellier (HSM) laboratory of the University of Montpellier (France). Both are used for validating altimetry-based water level and discharge.

4. Methods

4.1. Altimetry-Based Water Levels

Initially developed to provide accurate measurements of the sea surface topography, radar altimetry is now commonly used for the monitoring of inland water levels (see [8] for a recent review). The variations of the altimeter height from one cycle to the other can be associated to changes in water level.

In this study, we used the Multi-mission altimetry Processing Software (MAPS), frequently used for processing altimetry data over land and ocean (e.g., [36–40]), that allows a refined selection of the valid altimeter data to build time-series of water levels at a so-called virtual station. Data processing is composed of four main steps:

- (i) the rough delineation of the cross-section between the altimeter tracks and the rivers using Google Earth,
- (ii) the loading of the altimetry over the study area and the computation of the altimeter heights from the raw data contained in the GDRs,
- (iii) a refined selection of the valid altimetry data through visual inspection,
- (iv) the computation of the water level time-series as the median of the selected water levels every cycle.

A detailed description of the processing of altimetry data using MAPS can be found in [41]. MAPS is made available by CTOH. Previous studies showed that Ice-1-derived altimetry heights are the more suitable for hydrological studies in terms of accuracy of water levels and availability of the data (e.g., [13,37]) among the commonly available retracked data present in the GDRs. In this study, the data used were processed using the Offset Center of Gravity (OCOG) [42] also named Ice-1 or Ice retracking algorithm depending on the mission for all the missions.

Time series of water levels are generally obtained processing data from altimetry missions with a repeat period between 10 and 35 days [8]. It is what was done in this study to build the network of altimetry virtual stations under Jason-1/2/3, ERS-2/ENVISAT/SARAL and Sentinel-3A groundtracks. Considering the life cycles of these different missions and excluding the Jason missions whose crosstrack is too coarse (315 km at the Equator) to allow the definition of a dense network of virtual stations in, most of the river basins, there is a lack of data between the end of the ENVISAT mission in October 2010 on the nominal orbit, or in April 2012 considering its extended orbit, and the launch of the SARAL mission in February 2013. The only option to fill this gap is to consider the data acquired by the Cryosat-2 mission. Due to its long revisit time (369 days), its data are used to retrieve time series of water levels over large lakes [43], but are generally considered useless to define virtual

stations over rivers [44,45]. The long repeat cycle of Cryosat-2 is compensated by a small crosstrack of 7.5 km at the Equator leading to a large number of cross-sections between the river and the altimetry tracks in a close vicinity. Under the assumption that the temporality of water stages is not changing on a few tenths of kilometers of distance, it is possible to build VS gathering Cryosat-2 from tracks in a short distance thanks to the high spatial coverage and the sub-cycle period of 30 days of this mission. Changes in river characteristics (width, depth) over distances of a few kilometers are likely to impact the amplitude of the water stage but not its dynamics, a linear regression between altimetry-based water levels and in-situ data was applied to altimetry data to retrieve time series of water levels (see (2) in sub-section 4.2 Conversion into river discharges).

4.2. Discharge Estimates

River discharge is classically estimated from water level measurements through a functional relationship between the two quantities known as stage-discharge rating or rating curve (Rantz et al., 1982). It has the following form:

$$Q(t) = \alpha(h(t) - h_0)^\beta \quad (1)$$

where Q is the river discharge, h the water level, h_0 the null-discharge elevation, and α and β are related to the geometry of the channel cross-section and to the friction coefficient modulating the discharge.

This technique have been successfully applied to estimate river discharge using altimetry-based water levels when it was possible to derive the rating curve a common period of observation. It permits to derive river discharge with accuracy better than 20% (e.g., [18–20,22,46–48]).

As the altimetry crossing over the river does not generally occur at the location of the in-situ station but several tenths of kilometers upstream or downstream, the flow cross-sectional area is likely to vary over these short distances. To avoid errors caused by these changes, previous studies used a linear regression between altimetry and in situ water levels (h_{alti} and h_{insitu} respectively) when the dynamic of the flow is quite similar (e.g., [20,46]):

$$h_{insitu} = ah_{alti} + b \quad (2)$$

where a and b are the coefficients of the linear regression that allows the radar altimetry data to exactly fit the variations from the in situ gauge used to estimate the river discharge.

5. Results

5.1. Altimetry-Based Network of Gauging Stations

An altimetry-based network of 34 virtual stations (VS) was defined across the Ogooué river and its major tributaries (Ivindo and Ngounie rivers in northeast and southwest of the ORB respectively). Water level time series were mostly derived from Envisat, Saral and Sentinel-3A observations. As ENVISAT and SARAL missions were orbiting on the same nominal orbit, 15 of them provide a pluri-annual record from June 2002 to October 2010 and from February 2013 to June 2016, one of them from June 2002 to October 2010 and one of them from February 2013 to June 2016. As this orbit was formerly used by ERS-2, this record was extended from May 1995 to July 2003 for the 6 VS located closer to the mouth. Due to the small width of the rivers in the upstream part of the ORB and the presence of topography, VS could not be defined 125 km upstream Lambaréné because of the narrow width of the Ogooué river and its surrounding rugged topography. This network is completed with 2 VS created using observations from Jason-2 (from July 2008 to August 2016) and Jason-3 (since January 2016). Due to the large cross-track of these missions (315 km at the Equator), very few cross-sections between the rivers and the altimeter ground tracks occur. The network was also completed by 11 VS defined under Sentinel-3A ground tracks, which was launched in February 2016. The locations of the VS from the different altimetry missions are presented in Figure 2 and Table 1.

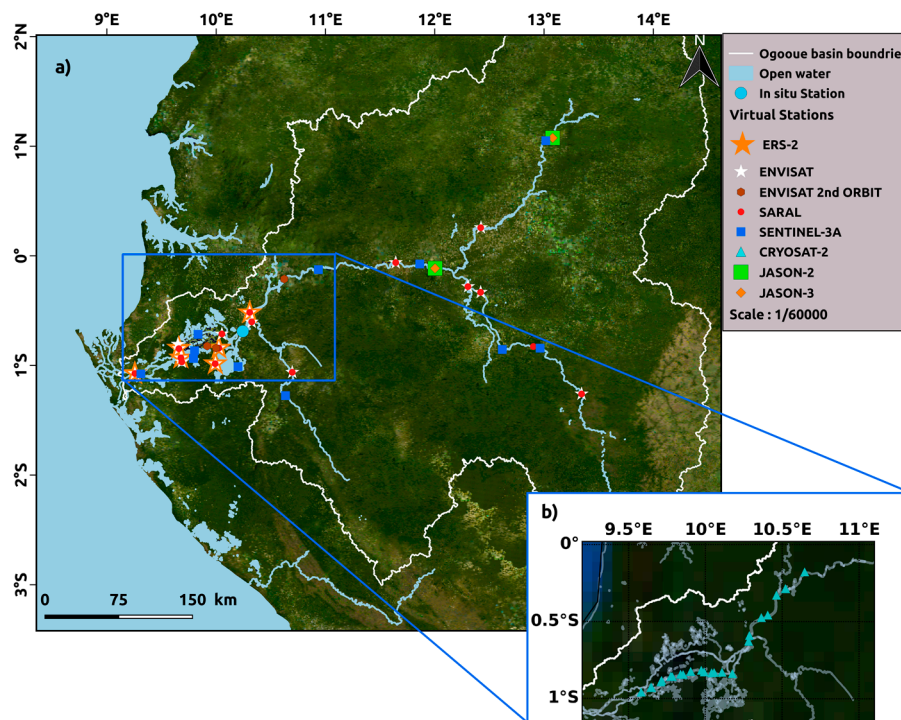


Figure 2. Locations of the altimetry virtual stations in the Ogooué River Basin. VS from ERS-2, ENVISAT, ENVISAT 2nd orbit, SARAL, Sentinel-3A, Cryosat-2, Jason-1, Jason-2, Jason-3 are represented using orange stars, white stars, brown dots, red dots, blue squares, cyan triangles, green squares and orange diamonds respectively. For readability purpose, virtual stations from missions with repeat period shorter than 35 days are presented in (a) and virtual stations from Cryosat-2 are presented in (b).

Table 1. List of VS where water stages are derived from altimetry measurements.

Virtual Stations	Missions	Longitude (°)	Latitude (°)	River Width (km)	Distance to the River Mouth (km)
SV_229_Ogooué	ENVISAT, SARAL	13.3533	−1.3082	0.22	693.09
SV_272_Ivindo	ENVISAT, SARAL	12.4228	0.2542	0.20	524.91
SV_272_Ogooué	ENVISAT, SARAL	12.3051	−0.2816	0.36	477.59
SV_315_Ogooué	ENVISAT, SARAL	11.6422	−0.0618	0.37	386.57
SV_358_Ngounié	ENVISAT, SARAL	10.6490	−1.2761	0.20	274.948
SV_401_Ngounié	ENVISAT, SARAL	10.3227	−0.5958	0.62	193.531
SV_401_Ogooué	ERS-2, ENVISAT, SARAL	10.3045	−0.5129	1.30	198.222
SV_444_Ogooué	ERS-2, ENVISAT, SARAL	9.2569	−1.0722	0.59	42.582
SV_730_Ogooué	SARAL	12.9154	−0.8316	0.19	607.233
SV_773_Ogooué	ENVISAT, SARAL	12.4700	−0.5595	0.23	494.696
SV_902_lake_Onangué	ERS-2, ENVISAT, SARAL	9.9912	−1.0001		160.97
SV_902_Ogooué	ERS-2, ENVISAT, SARAL	10.0280	−0.8323	1.25	141.66
SV_902_Ogooué_2	ENVISAT, SARAL	10.0551	−0.7091	0.32	152.215
SV_945_lake_Louandé	ENVISAT	9.6497	−0.8047		107.174
SV_945_lake_Ogognié	ENVISAT, SARAL	9.6844	−0.9624		101.671
SV_945_Ogooué	ERS-2, ENVISAT, SARAL	9.6755	−0.9220	1.19	97.413
SV_945_Ogooué_2	ERS-2, ENVISAT, SARAL	9.6571	−0.8382	0.47	103.125
Station 1	ENVISAT 2nd orbit	10.6414	−0.1864	0.49	127.826
Station 2	ENVISAT 2nd orbit	10.0208	−0.8328	0.88	138.166
Station 3	ENVISAT 2nd orbit	9.9445	−0.8082	1.17	252.246
SV_128_Ogooué	SENTINEL-3A	9.2788	−1.0638	1.23	45.271
SV_378_Ogooué	SENTINEL-3A	9.8069	−0.8454	1.24	112.654
SV_185_lake_Onangué	SENTINEL-3A	10.1962	−1.0009		169.463
SV_050_Ogooué	SENTINEL-3A	10.9045	−0.1177	0.30	298.329
SV_107_Ogooué	SENTINEL-3A	11.8457	−0.0803	0.37	412.048
SV_164_Ogooué	SENTINEL-3A	12.6126	−0.8438	0.31	564.01
SV_356_Ogooué	SENTINEL-3A	12.9676	−0.8423	0.30	617.561
SV_164_Ivindo	SENTINEL-3A	13.0280	1.0330	0.19	677.105
SV_050_Ngounié	SENTINEL-3A	10.6477	−1.2728	0.35	301.24

Table 1. Cont.

Virtual Stations	Missions	Longitude (°)	Latitude (°)	River Width (km)	Distance to the River Mouth (km)
SV_378_lake_Avanga	SENTINEL-3A	9.7878	−0.9345		112.299
SV_050_Ngounié Lambaréné	SENTINEL-3A CRYOSAT-2	9.8386 10.2220	−0.7021 −0.7139	0.23	301.24
SV_185_Ogooué	JASON-2, JASON-3	12.0035	−0.1148	0.36	430.318
SV_096_Ivindo	JASON-2, JASON-3	13.0790	1.0758	0.18	687.576

5.2. Altimetry-Based Water Levels Validation Using the Lambaréné Gauge Record

The network of gauge stations was not maintained after the 1980s in the ORB. Only the gauge station from Lambaréné provided measurements of water stages and discharge estimates during the period of acquisition of altimetry data. Four ERS-2/ENVISAT/SARAL tracks (401, 444, 902 and 945) are crossing the Ogooué River close to Lambaréné, at 22 and 135.5 km upstream and at 38 and 89 km downstream respectively. Sentinel-3 tracks 050, 128 and 378 are crossing the Ogooué River at 121 km upstream and 66 and 133 km downstream of Lambaréné respectively, as well as 32 Cryosat-2 tracks. Comparisons between altimetry-based and in situ water stages were performed for measurements acquired the same day. The results are presented in Figures 3–7 for ERS-2/ENVISAT/SARAL, Sentinel-3A and ENVISAT 2nd orbit and Cryosat-2 respectively. For the different missions except Cryosat-2, the water levels are presented from upstream (a) to downstream (c or d), (b) corresponding to the closest distance between the VS and the in situ station of Lambaréné.

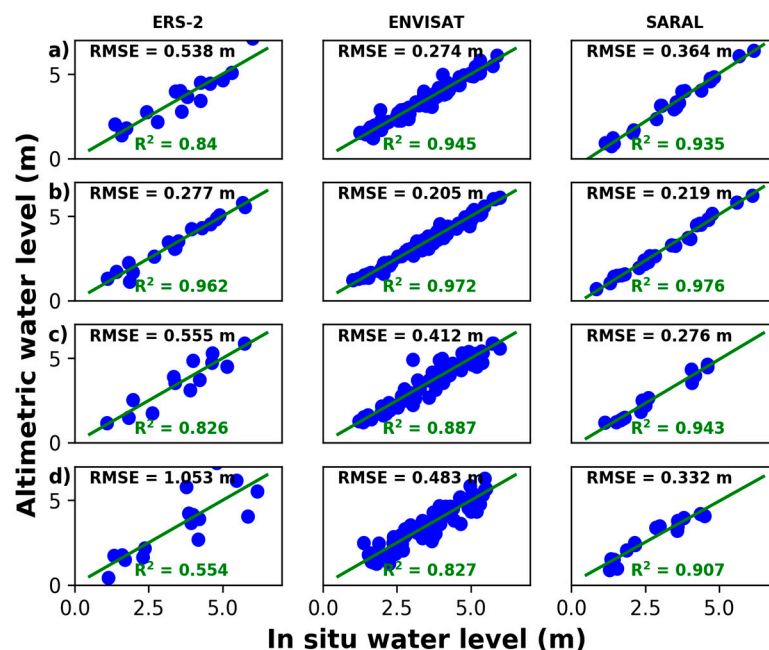


Figure 3. Results of the comparison between the altimetry-based water stages from ERS-2/ENVISAT/SARAL for tracks 401 (a), 902 (b), 945 (c), 444 (d) and the in situ ones from Lambaréné gauge station.

Overall very good results are obtained for all these stations. As expected, the quality of the water stage retrieval decreases as the distance to the in situ station increases. Better results were generally obtained using SARAL data, the first mission to operate in Ka-band, than using ERS-2 and ENVISAT ones (Ku-band, Figures 3 and 4). Results obtained using Sentinel-3A data, the first mission to operate in SAR mode on a frequent repetitive orbit, are very encouraging (Figure 5). In spite of the few cycles available (15), altimetry-based water levels obtained using data from this mission already exhibit a similar quality as the ones obtained using data from SARAL when considering the closer distance to the Lambaréné in situ station (Figure 5b). A very good agreement is also found with Cryosat-2 at the

Lambaréné ($R^2 = 0.96$ and $RMSE = 0.25$ m) demonstrating the potential of this mission for the retrieval of water stages (Figure 6).

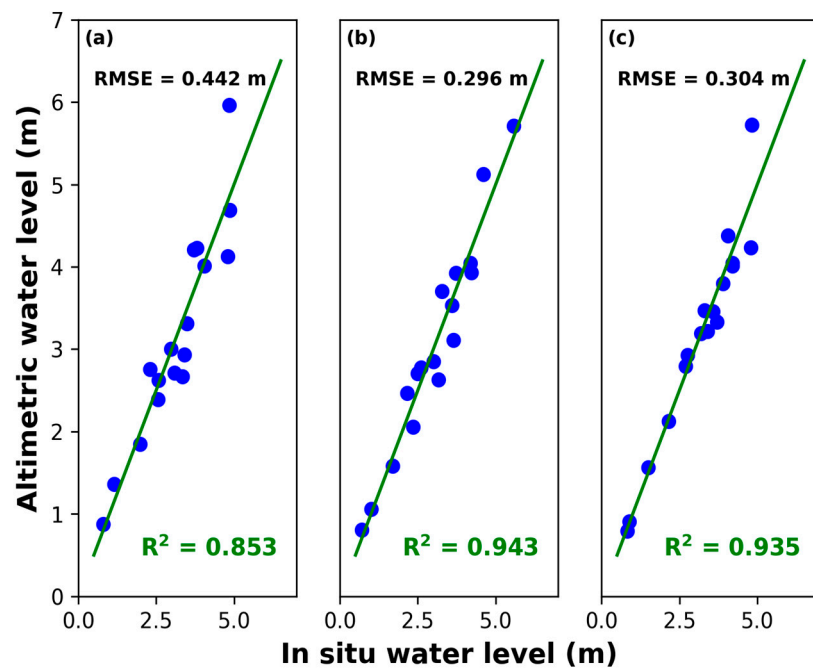


Figure 4. Results of the comparison between the altimetry-based water stages from ENVISAT on its second orbit for (a) Station 1, (b) Station 2 and (c) Station 3 and the in-situ ones from Lambaréné gauge station.

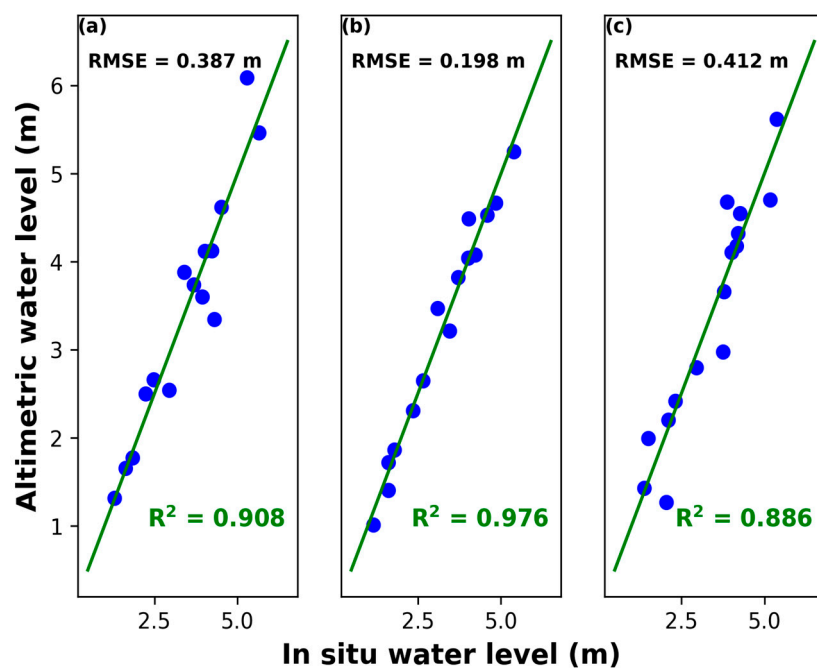


Figure 5. Results of the comparison between the altimetry-based water stages from Sentinel-3A for tracks (a) 050, (b) 378 and (c) 128 and the in-situ ones from Lambaréné gauge station.

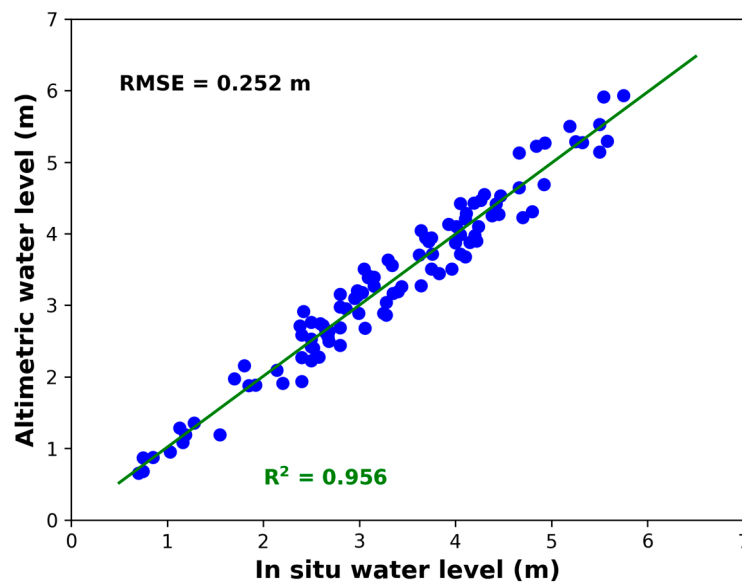


Figure 6. Results of the comparison between the altimetry-based water stages from Cryosat-2 and the in-situ ones from Lambaréné gauge station.

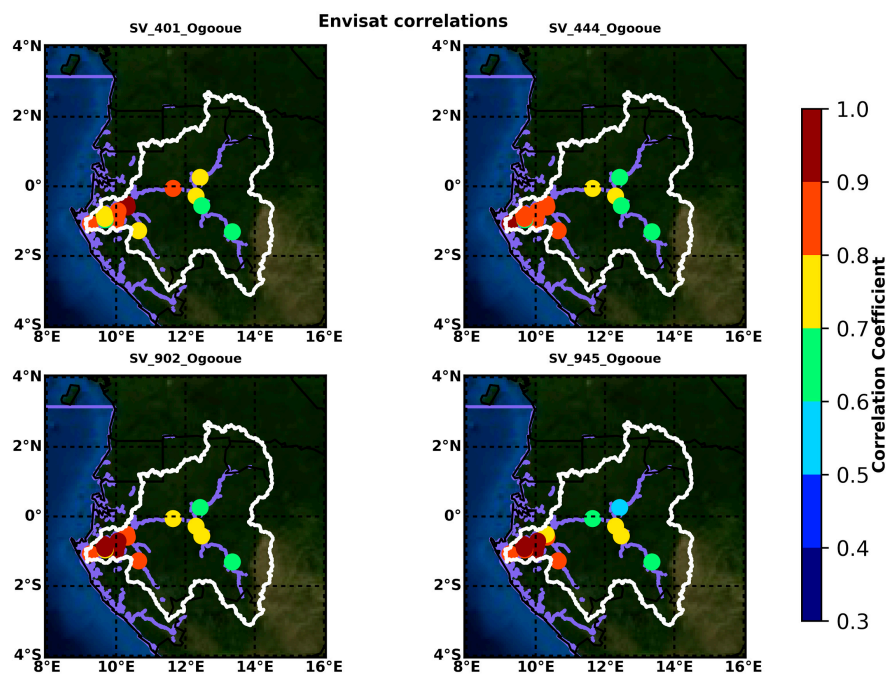


Figure 7. Maps of maximum of cross-correlation between time series from ENVISAT data in the ORB for the four VS around Lambaréné.

5.3. Consistency of the Altimetry-Based Water Levels in the Ogooué River Basin

Only one in-situ gauge station record had water stage measurements during the altimetry period in the ORB. Even if this record can be used to validate 4 SV from ERS-2/ENVISAT/SARAL, 3 from Sentinel-3A, and one combining Cryosat-2 water level estimates at different cross-sections, a consistency check was performed for the other stations in the ORB. It consists in estimating the cross-correlation between the different time-series of water levels from the same mission. Maxima of correlation were reported on Figures 6 and 7 for ENVISAT and SARAL respectively. As the repeat period of these mission is 35 days on their nominal orbit, only time-lags of plus or minus 53 days

(one repeat period and a half) were considered due to the relatively small scale of the ORB. Due to the changes of the river features (slope, depth, width, . . .), bias and RMSE were not computed between the time-series of altimetry-based water levels. This consistency-check was applied neither to the ERS-2 VS that are not sufficiently numerous (only 6 located on the downstream part of the river) nor to the ENVISAT VS from the second orbit because of the short period of operation of ENVISAT (17 cycles available).

It can be seen that maximum values of cross-correlation between the time series are greater downstream than upstream of the ORB whatever the VS considered to make the comparisons (Figures 7 and 8). Larger maxima of cross-correlation are obtained with the ENVISAT mission than with the SARAL mission. They are above 0.7 between ENVISAT VS in the downstream part of the basin up to the confluence between its two major tributaries, the Ivindo and the Ngounié Rivers. On these two tributaries, the maximum of cross-correlations generally range from 0.6 to 0.8 (Figure 7). Much lower agreement was found between the SARAL VS. If maxima of cross-correlation are generally above 0.6 on the downstream part of the ORB but they rapidly decrease down to 0.4 upstream. Higher consistency is found using ENVISAT VS on a larger part of the ORB.

No time-lag is present in most of the cases. Nevertheless, a few maxima cross-correlation coefficients between time series occurred with a time-lag of one month, for both ENVISAT and SARAL missions. This situation happened in the case of two stations located upstream of the Ogooué River (ENVISAT SV_229_Ogooué using SV_401_Ogooué, SV_902_Ogooué and SV_945_Ogooué validated against records from Lambaréné in situ gauge as reference and SARAL SV_773_Ogooué using SV_401_Ogooué and SV_945_Ogooué as reference) and in the case of the station SV_945_Lake_Ogognié located on the Lake Ogognié downstream of the ORB in cross-correlation with the validated time series from SV_401_Ogooué.

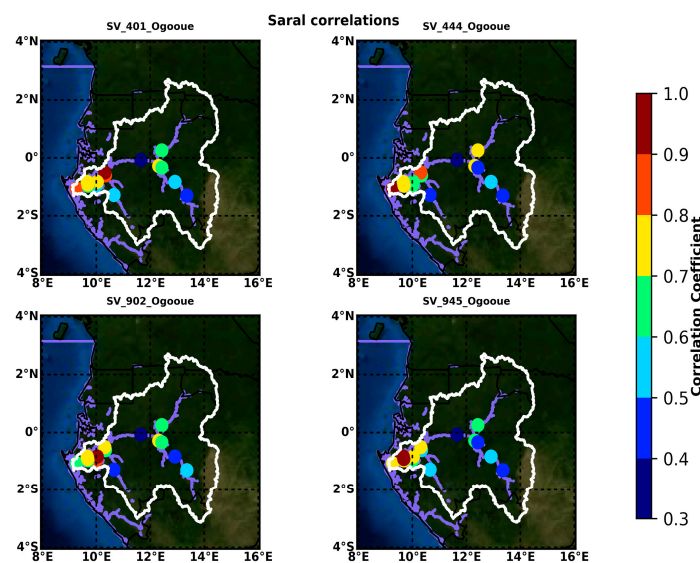


Figure 8. Maps of maximum of cross-correlation between time series from SARAL data in the ORB for the four VS around Lambaréné.

Due to the lack of in situ gauge station in the ORB with the exception of the one from Lambaréné, no validation was performed for the water stages derived from Jason-2 and Jason-3 data. As the two cross-sections between Jason-2 and 3 ground-tracks (185 on the Ogooué and 096 on the Ivindo) are close from cross-sections between Sentinel-3A ground-tracks (107 on the Ogooué and 164 on the Ivindo) (see Table 1 and Figure 2), cross-comparisons between the water levels derived from Jason-2, Jason-3 and Sentinel-3A were performed during the common period of availability of the different datasets. For this purpose, data from the 10-day repeat orbit missions (Jason-2 and Jason-3 that were

orbiting 2 minutes apart) were interpolated at the date of acquisition of Sentinel-3A. In both cases, Jason-2 time-series of water levels exhibit a clear seasonal cycle, especially for track 096 on the Ivindo, with high stages observed during the primary peak from October to December and the secondary peak in April-May and low stages observed in January-February (small dry season) and from June to August for the large dry season, which is consistent our knowledge of the hydrological cycle in the ORB (Figure 9). This also the case for Jason-3 time-series that agree well with the ones from Jason-2 ($R = 0.88$ and 0.87 and $RMSE = 0.51$ and 0.68 m for tracks 185 on the Ogooué and 096 on the Ivindo respectively). If similar but smoother water levels variations were observed in the Ivindo at the SV built under Sentinel-3A track 164 ($R = 0.92$ and 0.95 , $RMSE = 0.71$ and 0.56 m, Figure 9a), no realistic water level variations were observed at the SV built under Sentinel-3A track 107 (Figure 9b). This SV was discarded.

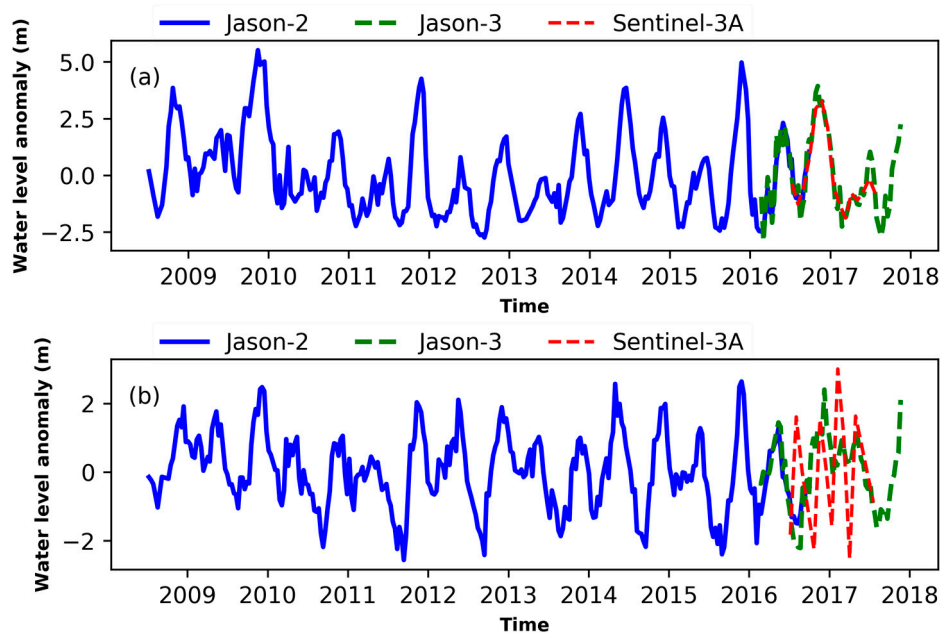


Figure 9. Time series of water level from Jason-2 (blue), Jason-3 (dashed green) and Sentinel-3A (dashed red) on the Ivindo (a) and upstream Ogooué (b) rivers.

5.4. Multi-Mission Discharge Estimates

The time-series of water level from the VS, that were validated against the stage record from the Lambaréné in situ gauge, were combined using Equation (2) to form a unique time series over May 1995–July 2017 time period. It is presented in Figure 10 along with the time-series of water levels from Lambaréné gauge station. The combined altimetry-based time series of water levels is in good agreement with the in-situ one ($R^2 = 0.96$ and $RMSE = 0.38$ m). Contrary to the individual altimetry-based time-series of water levels used in this study that are constrained by the revisit time of the satellite (27 days for ENVISAT on its second orbit, 35 days for ERS-2/ENVISAT and SARAL on their nominal orbit, 369 days for Cryosat-2), the combined time-series present the advantage to have between 3 to 4 (during the ERS-2 and the ENVISAT periods between 1995 and 2010) and 9 (during the SARAL and the Sentinel-3A periods since 2013 when combining with the Cryosat-2 measurements available since 2010) measurements each month.

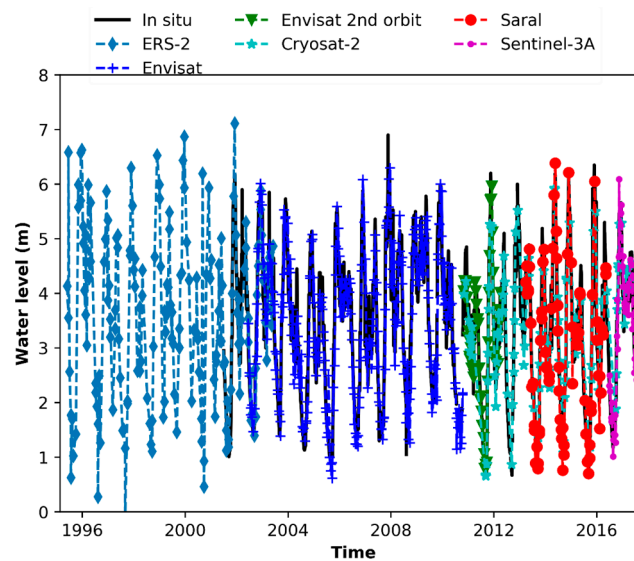


Figure 10. Time series of water level at Lambaréné from the in-situ gauge record (black continuous line), the multi-mission altimetry-based record (ERS-2 data are represented with diamonds, ENVISAT with blue crosses on its nominal orbit and with green triangles on its second orbit, Cryosat-2 with green-blue stars, SARAL with red circles, Sentinel-3 with purple dots).

Applying the rating curve relating water stages and discharge, established for the Lambaréné gauge using in situ measurements of water levels and discharge, an altimetry-based time series of discharge was obtained. Figure 11 shows discharges estimated from altimetry-based and in situ water levels at Lambaréné. A very good agreement between both sources ($R = 0.94$ and $RMSE = 701.6 \text{ m}^3 \cdot \text{s}^{-1}$ for a mean annual discharge of $4253.4 \text{ m}^3 \cdot \text{s}^{-1}$ or 16.5% of the mean annual discharge over the observation period). Considering the total annual discharge over the common observation period, altimetry-based and in situ estimates only differs by $1.4 \text{ m}^3 \cdot \text{s}^{-1}$ (or 0.03% of the mean annual discharge) in average (Table 2).

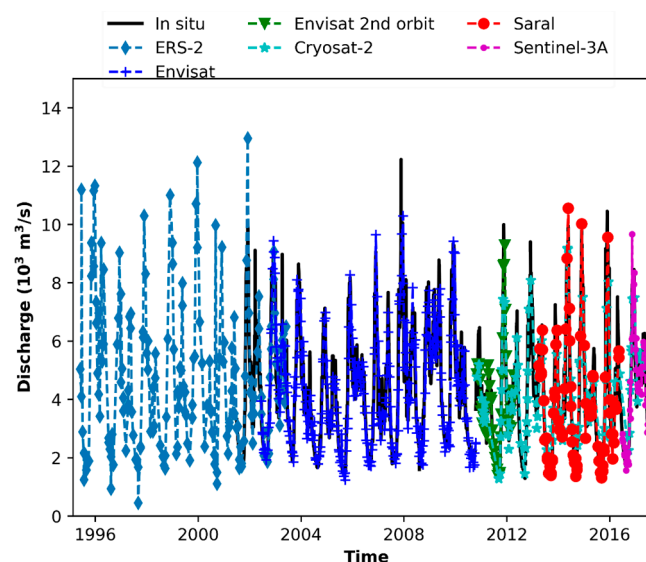


Figure 11. Time series of river discharge at Lambaréné from the in-situ gauge record (black continuous line), the multi-mission altimetry-based record (ERS-2 data are represented with diamonds, ENVISAT with blue crosses on its nominal orbit and with green triangles on its second orbit, Cryosat-2 with green-blue stars, SARAL with red circles, Sentinel-3 with purple dots).

Table 2. Average annual flow derived for the different VS of every altimetry mission and also combining their different records.

Missions	Stations	Estimated Discharge ($\text{m}^3 \cdot \text{s}^{-1}$)	Relative Error (%)	R(-)	RMSE ($\text{m}^3 \cdot \text{s}^{-1}$)
In situ	Lambaréné	4253.427	0	1	0
ERS-2	SV_401_Ogooué	4951.475	16.41	0.850	1107.647
	SV_444_Ogooué	5465.756	21.45	0.141	2466.262
	SV_902_Ogooué	4498.633	5.76	0.987	332.152
	SV_945_Ogooué	5104.026	19.99	0.886	920.226
	Combined	4848.378	13.99	0.755	1440.860
ENVISAT	SV_401_Ogooué	4311.470	1.36	0.969	431.757
	SV_444_Ogooué	4281.369	0.66	0.884	804.946
	SV_902_Ogooué	4316.212	1.47	0.981	352.028
	SV_945_Ogooué	4342.597	2.09	0.922	722.334
	Combined	4340.594	2.049	0.942	604.321
SARAL	SV_401_Ogooué	3927.343	-7.67	0.975	470.446
	SV_444_Ogooué	3103.856	-27.023	0.947	409.759
	SV_902_Ogooué	3851.170	-9.46	0.986	346.980
	SV_945_Ogooué	2898.672	-31.85	0.973	335.693
	Combined	4060.427	-4.537	0.978	396.820
ENVISAT 2nd Orbit	Station 1	3850.274	-9.47	0.816	868.273
	Station 2	3740.297	-12.06	0.963	450.838
	Station 3	3841.379	-9.69	0.895	654.027
	Combined	3839.296	-9.736	0.898	679.496
SENTINEL-3A	SV_050_Ogooué	4454.109	4.72	0.915	757.845
	SV_378_Ogooué	4210.519	-1.01	0.983	316.740
	SV_128_Ogooué	4373.213	2.82	0.931	629.888
	Combined	4262.683	0.22	0.942	597.610
CRYOSAT-2	Lambaréné	4188.220	-1.53	0.971	408.739
SENTINEL-3A + CRYOSAT-2	Combined	4118.9275	-3.162	0.967	462.141
CRYOSAT-2 + SARAL	Combined	4136.3508	-2.752	0.977	405.978
CRYOSAT-2 + ENVISAT 2nd orbit	Combined	4243.2487	-0.239	0.956	515.057
All missions	Combined	4252.052	-0.03	0.936	701.645

6. Discussion

Despite the relatively small size of the ORB and the small length of the Ogooué River (~900 km), the distance between Equatorial cross-tracks of the missions (80 km for ERS-2/ENVISAT/SARAL, and 315 km for Topex-Poseidon/Jason-1/Jason-2/Jason-3 on their nominal orbits), make possible the construction of a dense network of altimetric VS. It is composed of 16 SV using ENVISAT and SARAL, 6 SV using ERS-2 data, 10 SV using Sentinel-3A data, and only 2 SV using Jason-2 and Jason-3 data. In spite of the improvements made in the processing of data from early high precision missions, too few valid data were found in the GDR E data for Jason-1 to provide a continuous monitoring of water stages at two locations where the SV were constructed. These two cross-sections are located in the upstream parts of the basin where the river widths are between 180 and 360 m. Similarly, even if a very good agreement was found between ERS-2 based water levels in the downstream part of the basin, up to several tenths of kilometers upstream Lambaréné in situ station, no SV was defined either on the upstream Ogooué River or on its tributaries. Due to the small width of the river and the presence of higher topography, ERS-2 was affected more by tracking loss than ENVISAT. Furthermore, the accuracy of the data was degraded due to more frequent changes of acquisition modes than ENVISAT (Table 3). ENVISAT was, most of the time, operating in the 320 MHz Ku chirp bandwidth acquisition mode than in the 80 MHz or the 20 MHz modes, that is to say with the better range resolution as the size of the range detection window is 64, 256 and 1024 m respectively. For ERS-2, different cases were observed.

When no valid water level time series were obtained from ERS-2 acquisitions, it can be attributed to either rapid changes in the topography along the track causing changes in Ku chirp bandwidth acquisition modes (with a large number of acquisitions at 82.5 MHz causing a loss of accuracy of the data) or altimeter lock on the hills on top of the river (with acquisitions mostly at 330 MHz but a few tenths of meters above the river, see the example presented in [37] for ENVISAT). When time-series of water levels were derived, the percentage of acquisition at high frequency is high but lower than the one for ENVISAT causing a loss of accuracy compared with ENVISAT (Table 1).

Compared to earlier missions on the same nominal orbit operating at Ku-band (ERS-2 and ENVISAT), SARAL, the first mission to operate at Ka-band, agrees better with gauge records. Higher R and lower RMSE were found between the time-series of water stages from in-situ and from altimetry-based measurements for the four SV close to Lambaréné (Figure 3). In spite of the short period of observation of SARAL on its nominal orbit (35 cycles from February 2013 to June 2016 and even shorter considering that SARAL started to drift since July 2016), the benefits of the Ka-band smaller footprint compared to the Ku-one can be clearly observed as it was reported in other locations [49]. The use of other cycles would have led to large errors in the water stage retrievals because of (i) slope effects causing large changes of water base levels, (ii) changes in the characteristics of the river (width, depth) responsible changes in amplitude of the water levels, (iii) detection of other water bodies (e.g., lakes) than the Ogooué River.

Only considering ERS-2, ENVISAT and SARAL on their nominal orbit would have resulted in gaps in the monitoring of water levels in the ORB between October 2010 and February 2013 and after July 2016, and especially in Lambaréné where the river discharge is estimated. To complete the time-series, data from the ENVISAT 2nd orbit were considered from October 2010 to April 2012. Three SV were build giving water estimates of equivalent quality as the ones obtained on the nominal orbit (Figure 4). Applying an innovative processing, time-series of water levels were derived from Cryosat-2 measurements, the first altimetry mission to operate in SAR mode. The results show, that the data from this mission, that are of very good quality (R^2 and RMSE of very similar quality as ENVISAT or SARAL, see Figure 6). The monitoring of the water levels in the Ogooué can continue using acquisitions from the Sentinel-3A mission and soon, from the Sentinel-3B. Comparisons performed against the in-situ gauge records from Lambaréné of one year and a half of Sentinel-3A-based water levels show the high quality of the data acquired in SAR mode ($R^2 = 0.98$ and $RMSE < 20$ cm for the SV located at the closer distance to Lambaréné station, see Figure 5).

Table 3. Acquisition modes of the ERS-2 and ENVISAT measurements for the VS in the ORB.

Virtual Stations	Rivers or Lakes	Missions	ENVISAT Data Modes			ERS-2 Data Modes	
			320 Hz (%)	80 Hz (%)	20 Hz (%)	330 Hz (%)	82.5 Hz (%)
SV_229_Ogooué	Ogooué	ENVISAT, SARAL	99.786	0.213	0	100	0
SV_272_Ivindo	Ivindo	ENVISAT, SARAL	96.893	1.804	1.302	58.0	42.0
SV_272_Ogooué	Ogooué	ENVISAT, SARAL	98.267	0.533	1.2	6.25	93.75
SV_315_Ogooué	Ogooué	ENVISAT, SARAL	91.896	6.212	1.890	100	0
SV_358_Ngounié	Ngounié	ENVISAT, SARAL	88.76	10.3	0.939	70.270	29.729
SV_401_Ngounié	Ngounié	ENVISAT, SARAL	98.776	1.146	0.077	81.132	18.867
SV_401_Ogooué	Ogooué	ERS-2, ENVISAT, SARAL	98.776	1.146	0.077	81.132	18.867
SV_444_Ogooué	Ogooué	ERS-2, ENVISAT, SARAL	99.887	0.113	0	85.0	15.0
SV_730_Ogooué	Ogooué	SARAL	92.347	6.152	1.5005	34.426	65.573
SV_773_Ogooué	Ogooué	ENVISAT, SARAL	99.178	0.821	0	70.588	29.411
SV_902_lake_Onangué	lake Onangué	ERS-2, ENVISAT, SARAL	99.669	0.259	0.070	87.804	12.195
SV_902_Ogooué	Ogooué	ERS-2, ENVISAT, SARAL	99.669	0.259	0.070	87.804	12.195
SV_902_Ogooué_2	Ogooué	ENVISAT, SARAL	99.669	0.259	0.070	87.804	12.195
SV_945_lake_Louandé	lake Louandé	ENVISAT	99.513	0.487	0	100	0
SV_945_lac_Ogognié	lake Ogognié	ENVISAT, SARAL	99.513	0.487	0	100	0
SV_945_Ogooué	Ogooué	ERS-2, ENVISAT, SARAL	99.513	0.487	0	100	0
SV_945_Ogooué_2	Ogooué	ENVISAT	99.513	0.487	0	100	0

Due to the presence of only one in-situ station with records during the altimetry acquisition period, the consistency of the altimetry-based time-series of water levels was checked for ENVISAT and SARAL through cross-correlation estimates. They were performed choosing as reference the SV close to Lambaréné station whose records were validated. The difference observed for the cross-correlations between ENVISAT and SARAL occur in the upstream parts of the basin (Figures 7 and 8 respectively). The lower scores for SARAL can be attributed to the shorter observation period of SARAL compared with ENVISAT (35 cycles for SARAL against 85 for ENVISAT, that is to say, more or less a ratio of one third). This difference in number of observations has a smaller impact on the downstream part of the ORB as the water stages are mostly driven by the flow from the upstream parts. On the upstream part, changes in rainfall conditions between two VS are likely to strongly modify the water stage at these two locations. Even a few of this kind of changes can reduce the correlation between the two time-series of river levels between these two stations, especially for shorter records. Due to the relatively small length of the basin and the quite long repeat period of ENVISAT and SARAL (35 days), maxima of correlation are generally observed with no time-lag, except for a limited number of stations in the upstream parts of the ORB where differences lower than one month were obtained.

Based on the good agreement found between in situ and altimetry-based water stages for the VS located around Lambaréné gauge station, the stage discharge rating curve was applied to any individual VS but also for the combination of VS for the same mission. The results are presented in Table 2. This combination represents a good compromise between quality of the resulting time series of discharge and number of observations. For all the missions, the results of the combination are very close to the best result obtained with a single one. It also decreases the risk to miss a rapid flood event that will modify the annual discharge. The combination of data from several missions (ENVISAT 2nd orbit + Cryosat-2, SARAL + Cryosat-2, Sentinel-3A + Cryosat-2) also increase the quality of the discharge estimate. When combining the data from the missions (Cryosat-2 period of availability of the data is overlapping the ones from ENVISAT, ENVISAT 2nd orbit, SARAL and Sentinel-3A), very good performances are obtained (see Table 2).

7. Conclusions

This study provides one of the first assessments of the performances of multiple satellite altimetry-based water levels in a river basin, from ERS-2 to Sentinel-3A. Comparisons between altimetry water stages and in situ gauge records from Lambaréné, the unique station still in operation in the ORB showed the improvement in performances of the missions in operation since ERS-2. In spite of good performances in the downstream part of the ORB ($R^2 > 0.82$ and $RMSE < 0.6$ m for 3 of the four comparisons), no VS using ERS-2 data were created in the upstream part of the basin due to the small width of the rivers and the presence of topography. On the contrary, the whole basin was sampled using ENVISAT ($R^2 > 0.82$ and $RMSE < 0.5$ m) and SARAL ($R^2 > 0.90$ and $RMSE < 0.4$ m) on the same orbit. A very good consistency was also found for these two missions when computing cross-correlations between altimetry-based water stages all over the basin. As SARAL orbit control was not as strict as is generally is for high precision altimetry missions, the drifts of several kilometers from the nominal paths lead to lower agreement in the upstream parts of the basin than using ENVISAT. Missions operating in SAR mode also exhibit very good accuracy ($R^2 > 0.88$ and $RMSE < 0.4$ m for only one year and a half of Sentinel-3A data and $R^2 = 0.96$ and $RMSE = 0.25$ m for Cryosat-2). For Cryosat-2, the concept of VS was extended: data acquired on close cross-sections were combined to build the time series of water level. The use of Cryosat-2 (and ENVISAT 2nd orbit) data allowed a continuous monitoring of the ORB for all the altimetry period, showing the potential of the data acquired during geodetic (drifting) orbit of the altimetry missions for land hydrology.

The altimetry-based time-series of water levels from the different altimetry missions close to the Lambaréné in situ stations were converted to discharges using the rating curves from the in situ station. Very good agreement was also found, the quality of which is directly linked to the accuracy of the water levels at the VS for the different missions. This study also shows the interest to combine the

data from different missions to improve quality of the monitoring of level and discharge in terms of sampling frequency and annual discharge estimates.

The network of altimetry VS built in this study and associated discharge estimates has a strong interest for the scientific community. It will allow (i) the continuous monitoring of water stages in an almost ungauged basin, (ii) the analysis of possible effects of climate variability and anthropogenic effects (i.e., deforestation) on the hydrological cycle of the ORB. It will be very useful for the calibration and validation of the NASA/CNES Surface Water and Ocean Topography (SWOT) mission, that will use the SAR interferometry technique to map surface water elevation at a spatial resolution of 100 m as its one day calibration orbit encompass the downstream part of the Ogooué Basin.

Acknowledgments: This work is dedicated to Gaston Liéno who sadly passed away in 2015. He enormously contributed to the continuity of study operations in the Ogooué river basin. The authors are grateful to the Center for Topographic studies of the Ocean and Hydrosphere (CTOH) at LEGOS (Toulouse, France) for providing the altimetry dataset. We also thank the Société de l'Énergie et de l'Eau du Gabon (SEEG) branch of Lambaréné (Lambaréné, Gabon) for supplying of the Ogooué water level from the Lambaréné hydrological station. Aurélie Flore KOUMBA PAMBO, Scientific Cell coordinator, Agence Nationale des Parcs Nationaux (ANPN) and Centre National de la Recherche Scientifique et Technologique (CENAREST), Libreville, Gabon, is warmly thanked for her assistance with respect to the research authorizations. Other thanks go to the "Service Coopération et de l'Action Culturelle (SCAC)" of the French Embassy in Cameroon and TNC-Gabon, and the project "Centre de Topographie des Océans et de l'Hydrosphère" funded by CNES. This work was supported by the French national programme EC2CO-Biohefect "Régime d'Altération/Érosion en Afrique Centrale (RALTERAC)". Final acknowledgements are for the project "Jeune Equipe Associée Internationale—Réponse du Littoral Camerounais aux Forçages Océaniques Multi-Échelles (JEA-RELIFOME)" of the University of Douala and the Laboratoire Mixte International (LMI) Dynamique des écosystèmes continentaux d'Afrique Centrale en contexte de changements globaux (DYCOFAC) for its support in the accomplishment of this work. The authors want to thank two anonymous Reviewers for their helpful comments.

Author Contributions: Sakaros Bogning and Frédéric Frappart conceived and designed the study; Sakaros Bogning performed the altimetry data processing with the help of Fabien Blarel, Frédéric Frappart, Fernando Niño and Frédérique Seyler; Jean-Pierre Briquet and Gil Mahé processed the in situ data; all the authors analyzed the results and contributed to the writing of the paper.

Conflicts of Interest: The authors declare no conflict of interest.

References

1. Younger, P.L. *Water*; Hodder & Stoughton: London, UK, 2012.
2. Vörösmarty, C.J.; Green, P.; Salisbury, J.; Lammers, R.B. Global water resources: Vulnerability from climate change and population growth. *Science* **2000**, *289*, 284–288. [[CrossRef](#)] [[PubMed](#)]
3. Oki, T.; Kanae, S. Global hydrological cycles and world water resources. *Science* **2006**, *313*, 1068–1072. [[CrossRef](#)] [[PubMed](#)]
4. Gleick, P.H. Global freshwater resources: Soft-path solutions for the 21st century. *Science* **2003**, *302*, 1524–1528. [[CrossRef](#)] [[PubMed](#)]
5. Alsdorf, D.E.; Rodríguez, E.; Lettenmaier, D.P. Measuring surface water from space. *Rev. Geophys.* **2007**, *45*, RG2002. [[CrossRef](#)]
6. Alsdorf, D.; Beighley, E.; Laraque, A.; Lee, H.; Tshimanga, R.; O'Loughlin, F.; Mahé, G.; Dinga, B.; Moukandi, G.; Spencer, R.G.M. Opportunities for hydrologic research in the Congo Basin. *Rev. Geophys.* **2016**, *54*, 378–409. [[CrossRef](#)]
7. Stammer, D.; Cazenave, A. *Satellite Altimetry over Oceans and Land Surfaces*; Taylor & Francis: Boca Raton, FL, USA, 2017.
8. Crétaux, J.-F.; Nielsen, K.; Frappart, F.; Papa, F.; Calmant, S.; Benveniste, J. Hydrological applications of satellite altimetry: Rivers, lakes, man-made reservoirs, inundated areas. In *Satellite Altimetry over Oceans and Land Surfaces*; Stammer, D., Cazenave, A., Eds.; Earth Observation of Global Changes; CRC Press: Boca Raon, FL, USA, 2017; pp. 459–504.
9. Morris, C.S.; Gill, S.K. Variation of Great Lakes water levels derived from Geosat altimetry. *Water Resour. Res.* **1994**, *30*, 1009–1017. [[CrossRef](#)]
10. Birkett, C.M. The contribution of TOPEX/POSEIDON to the global monitoring of climatically sensitive lakes. *J. Geophys. Res.* **1995**, *100204*, 179–225. [[CrossRef](#)]

11. Koblinsky, C.J.; Clarke, R.T.; Brenner, A.C.; Frey, H. Measurement of river level variations with satellite altimetry. *Water Resour. Res.* **1993**, *29*, 1839–1848. [[CrossRef](#)]
12. Birkett, C.M. Contribution of the TOPEX NASA Radar Altimeter to the global monitoring of large rivers and wetlands. *Water Resour. Res.* **1998**, *34*, 1223. [[CrossRef](#)]
13. Frappart, F.; Calmant, S.; Cauhopé, M.; Seyler, F.; Cazenave, A. Preliminary results of ENVISAT RA-2-derived water levels validation over the Amazon basin. *Remote Sens. Environ.* **2006**, *100*, 252–264. [[CrossRef](#)]
14. Baup, F.; Frappart, F.; Maubant, J. Use of satellite altimetry and imagery for monitoring the volume of small lakes. In Proceedings of the International Geoscience and Remote Sensing Symposium (IGARSS), Quebec City, QC, Canada, 13–18 July 2014.
15. Sulistioadi, Y.B.; Tseng, K.-H.; Shum, C.K.; Hidayat, H.; Sumaryono, M.; Suhardiman, A.; Setiawan, F.; Sunarso, S. Satellite radar altimetry for monitoring small rivers and lakes in Indonesia. *Hydrol. Earth Syst. Sci.* **2015**, *19*, 341–359. [[CrossRef](#)]
16. Frappart, F.; Papa, F.; Malbeteau, Y.; León, J.G.; Ramillien, G.; Prigent, C.; Seoane, L.; Seyler, F.; Calmant, S. Surface freshwater storage variations in the orinoco floodplains using multi-satellite observations. *Remote Sens.* **2015**, *7*, 89–110. [[CrossRef](#)]
17. Bjerklie, D.M.; Lawrence Dingman, S.; Vorosmarty, C.J.; Bolster, C.H.; Congalton, R.G. Evaluating the potential for measuring river discharge from space. *J. Hydrol.* **2003**, *278*, 17–38. [[CrossRef](#)]
18. Kouraev, A.V.; Zakharova, E.A.; Samain, O.; Mognard, N.M.; Cazenave, A. Ob' river discharge from TOPEX/Poseidon satellite altimetry (1992–2002). *Remote Sens. Environ.* **2004**, *93*, 238–245. [[CrossRef](#)]
19. Zakharova, E.A.; Kouraev, A.V.; Cazenave, A.; Seyler, F. Amazon River discharge estimated from TOPEX/Poseidon altimetry. *Comptes Rendus Geosci.* **2006**, *338*, 188–196. [[CrossRef](#)]
20. Papa, F.; Durand, F.; Rossow, W.B.; Rahman, A.; Bala, S.K. Satellite altimeter-derived monthly discharge of the Ganga-Brahmaputra River and its seasonal to interannual variations from 1993 to 2008. *J. Geophys. Res. Ocean.* **2010**, *115*, C12013. [[CrossRef](#)]
21. Birkinshaw, S.J.; Moore, P.; Kilsby, C.G.; O'Donnell, G.M.; Hardy, A.J.; Berry, P.A.M. Daily discharge estimation at ungauged river sites using remote sensing. *Hydrol. Process.* **2014**, *28*, 1043–1054. [[CrossRef](#)]
22. Leon, J.G.; Calmant, S.; Seyler, F.; Bonnet, M.-P.; Cauhopé, M.; Frappart, F.; Filizola, N.; Fraizy, P. Rating curves and estimation of average water depth at the upper Negro River based on satellite altimeter data and modeled discharges. *J. Hydrol.* **2006**, *328*, 481–496. [[CrossRef](#)]
23. Tarpanelli, A.; Barbetta, S.; Brocca, L.; Moramarco, T. River Discharge Estimation by Using Altimetry Data and Simplified Flood Routing Modeling. *Remote Sens.* **2013**, *5*, 4145–4162. [[CrossRef](#)]
24. Paris, A.; Dias de Paiva, R.; Santos da Silva, J.; Medeiros Moreira, D.; Calmant, S.; Garambois, P.-A.; Collischonn, W.; Bonnet, M.-P.; Seyler, F. Stage-discharge rating curves based on satellite altimetry and modeled discharge in the Amazon basin. *Water Resour. Res.* **2016**, *52*, 3787–3814. [[CrossRef](#)]
25. Wilson, M.D.; Bates, P.; Alsdorf, D.; Forsberg, B.; Horritt, M.; Melack, J.; Frappart, F.; Famiglietti, J. Modeling large-scale inundation of Amazonian seasonally flooded wetlands. *Geophys. Res. Lett.* **2007**, *34*. [[CrossRef](#)]
26. Getirana, A.; Bonnet, M.; Calmant, S.; Roux, E.; Rotunno Filho, O.C.; Mansur, W.J. Hydrological monitoring of poorly gauged basins based on rainfall-runoff modeling and spatial altimetry. *J. Hydrol.* **2009**, *379*, 205–219. [[CrossRef](#)]
27. Milzow, C.; Krogh, P.E.; Bauer-Gottwein, P. Combining satellite radar altimetry, SAR surface soil moisture and GRACE total storage changes for model calibration and validation in a large ungauged catchment. *Hydrol. Earth Syst. Sci. Discuss.* **2010**, *7*, 9123–9154. [[CrossRef](#)]
28. Pereira-Cardenal, S.; Riegels, N.D.; Berry, P.A.M.; Smith, R.G.; Yakovlev, A.; Siegfried, T.U.; Bauer-Gottwein, P. Real-time remote sensing driven river basin modeling using radar altimetry. *Hydrol. Earth Syst. Sci.* **2011**, *15*, 241–254. [[CrossRef](#)]
29. De Paiva, R.C.D.; Buarque, D.C.; Collischonn, W.; Bonnet, M.P.; Frappart, F.; Calmant, S.; Bulhões Mendes, C.A. Large-scale hydrologic and hydrodynamic modeling of the Amazon River basin. *Water Resour. Res.* **2013**, *49*, 1226–1243. [[CrossRef](#)]
30. Mignard, S.L.A.; Mulder, T.; Martinez, P.; Charlier, K.; Rossignol, L.; Garlan, T. Deep-sea terrigenous organic carbon transfer and accumulation: Impact of sea-level variations and sedimentation processes off the Ogooue River (Gabon). *Mar. Pet. Geol.* **2017**, *85*, 35–53. [[CrossRef](#)]
31. Mahe, G.; Lérique, J.; Olivry, J.-C. Le fleuve Ogooué au Gabon: Reconstitution des débits manquants et mise en évidence de variations climatiques à l'équateur. *Hydrol. Cont.* **1990**, *5*, 105–124.

32. Lambert, T.; Darchambeau, F.; Bouillon, S.; Alhou, B.; Mbega, J.D.; Teodoru, C.R.; Nyoni, F.C.; Massicotte, P.; Borges, A.V. Landscape Control on the Spatial and Temporal Variability of Chromophoric Dissolved Organic Matter and Dissolved Organic Carbon in Large African Rivers. *Ecosystems* **2015**, *18*, 1224–1239. [[CrossRef](#)]
33. Lienou, G.; Mahe, G.; Paturel, J.E.; Servat, E.; Sighomnou, D.; Ekodeck, G.E.; Dezetter, A.; Dieulin, C. Evolution des régimes hydrologiques en région équatoriale camerounaise: Un impact de la variabilité climatique en Afrique équatoriale? *Hydrol. Sci. J.* **2008**, *53*, 789–801. [[CrossRef](#)]
34. Home—CTOH. Available online: <http://ctoh.legos.obs-mip.fr/> (accessed on 24 October 2017).
35. Frappart, F.; Legrésy, B.; Niño, F.; Blarel, F.; Fuller, N.; Fleury, S.; Birol, F.; Calmant, S. An ERS-2 altimetry reprocessing compatible with ENVISAT for long-term land and ice sheets studies. *Remote Sens. Environ.* **2016**, *184*, 558–581. [[CrossRef](#)]
36. Blarel, F.; Frappart, F.; Legrésy, B.; Blumstein, D.; Fatras, C.; Mougin, E.; Papa, F.; Prigent, C.; Rémy, F.; Niño, F.; et al. Radar altimetry backscattering signatures at Ka, Ku, C and S bands over land. In Proceedings of the Living Planet Symposium, Prague, Czech Republic, 9–13 May 2016.
37. Biancamaria, S.; Frappart, F.; Leleu, A.-S.; Marieu, V.; Blumstein, D.; Desjonquères, J.-D.; Boy, F.; Sottolichio, A.; Valle-Levinson, A. Satellite radar altimetry water elevations performance over a 200 m wide river: Evaluation over the Garonne River. *Adv. Space Res.* **2017**, *59*, 128–146. [[CrossRef](#)]
38. Frappart, F.; Roussel, N.; Biancale, R.; Martinez Benjamin, J.J.; Mercier, F.; Perosanz, F.; Garate Pasquin, J.; Martin Davila, J.; Perez Gomez, B.; Gracia Gomez, C.; et al. The 2013 Ibiza Calibration Campaign of Jason-2 and SARAL Altimeters. *Mar. Geodesy* **2015**, *38*, 219–232. [[CrossRef](#)]
39. Vu, P.; Frappart, F.; Darrozes, J.; Marieu, V.; Blarel, F.; Ramillien, G.; Bonnefond, P.; Birol, F. Multi-Satellite Altimeter Validation along the French Atlantic Coast in the Southern Bay of Biscay from ERS-2 to SARAL. *Remote Sens.* **2018**, *10*, 93. [[CrossRef](#)]
40. Salameh, E.; Frappart, F.; Marieu, V.; Spodar, A.; Parisot, J.-P.; Hanquiez, V.; Turki, I.; Laignel, B. Monitoring Sea Level and Topography of Coastal Lagoons Using Satellite Radar Altimetry: The Example of the Arcachon Bay in the Bay of Biscay. *Remote Sens.* **2018**, *10*, 297. [[CrossRef](#)]
41. Frappart, F.; Papa, F.; Marieu, V.; Malbeteau, Y.; Jordy, F.; Calmant, S.; Durand, F.; Bala, S. Preliminary Assessment of SARAL/AltiKa Observations over the Ganges-Brahmaputra and Irrawaddy Rivers. *Mar. Geodesy* **2015**, *38*, 568–580. [[CrossRef](#)]
42. Wingham, D.J.; Rapley, C.G.; Griffiths, H. New Techniques in Satellite Altimeter Tracking Systems. In Proceedings of the International Geoscience and Remote Sensing Symposium (IGARSS), Zurich, Switzerland, 1986; pp. 1339–1344.
43. Nielsen, K.; Stenseng, L.; Andersen, O.; Knudsen, P. The Performance and Potentials of the CryoSat-2 SAR and SARIn Modes for Lake Level Estimation. *Water* **2017**, *9*, 374. [[CrossRef](#)]
44. Schneider, R.; Godiksen, P.N.; Villadsen, H.; Madsen, H.; Bauer-Gottwein, P. Application of CryoSat-2 altimetry data for river analysis and modelling. *Hydrol. Earth Syst. Sci.* **2017**, *21*, 751–764. [[CrossRef](#)]
45. Jiang, L.; Schneider, R.; Andersen, O.; Bauer-Gottwein, P. CryoSat-2 Altimetry Applications over Rivers and Lakes. *Water* **2017**, *9*, 211. [[CrossRef](#)]
46. Birkinshaw, S.J.; O'Donnell, G.M.; Moore, P.; Kilsby, C.G.; Fowler, H.J.; Berry, P.A.M.M. Using satellite altimetry data to augment flow estimation techniques on the Mekong River. *Hydrol. Process.* **2010**, *24*, 3811–3825. [[CrossRef](#)]
47. Papa, F.; Bala, S.K.; Pandey, R.K.; Durand, F.; Gopalakrishna, V.V.; Rahman, A.; Rossow, W.B. Ganga-Brahmaputra river discharge from Jason-2 radar altimetry: An update to the long-term satellite-derived estimates of continental freshwater forcing flux into the Bay of Bengal. *J. Geophys. Res. Ocean.* **2012**, *117*, C11021. [[CrossRef](#)]
48. Getirana, A.C.V.; Peters-Lidard, C. Estimating water discharge from large radar altimetry datasets. *Hydrol. Earth Syst. Sci.* **2013**, *17*, 923–933. [[CrossRef](#)]
49. Bonnefond, P.; Verron, J.; Aublanc, J.; Babu, K.; Bergé-Nguyen, M.; Cancet, M.; Chaudhary, A.; Crétaux, J.-F.; Frappart, F.; Haines, B.; et al. The Benefits of the Ka-Band as Evidenced from the SARAL/AltiKa Altimetric Mission: Quality Assessment and Unique Characteristics of AltiKa Data. *Remote Sens.* **2018**, *10*, 83. [[CrossRef](#)]

